A Methodology for Offshore Transmission System Optimization Considering Spacial Constraints

Stephen Hardy, Hakan Ergun, Dirk Van Hertem
ELECTA, Department of Electrical Engineering, KU Leuven, Leuven 3000, Belgium and EnergyVille, Genk, Belgium

***Abstract*—This work presents an optimization method for offshore wind transmission networks considering a three dimensional spacial representation of multiple onshore connection points, bathymetry and no-go zones. The model accounts for capital expenditures (CAPEX) as well as operational expenditures such as cable and transformer losses, corrective maintenance (CM) and expected energy not transmitted (EENT). For accurate determination of operational expenditures, time series of wind generation profiles are used. The methodology combines an original offshore substation (OSS) placement algorithm, a greedy search algorithm of the combinatorial search space and a mixed integer linear programming (MILP) model. Two simplifications of the full three dimensional spacial model are presented to increase tractability of large scale test cases. To demonstrate the utility of the approach, the model is applied to the Belgian Exclusive Economic Area (EEA). Results for the full three dimensional problem and the two simplified variations are compared in terms of solution quality and computation time.**

***Index Terms*—Offshore wind topology, greedy algorithm, mixed-integer optimization, offshore grid, transmission expansion planning, wind energy.**

Nomenclature

	Definition		Definition
b	Auxiliary bus.	$\boldsymbol{B}$	set of auxiliary buses.
$\mathbb{B}$	Binary decision variable.	$\boldsymbol{\mathcal{B}}$	Set of binary decision variables.
$\mathbb{C}$	Equipment cost.	$\boldsymbol{\mathcal{C}}$	Set of equipment costs.
c	A contingency.	C	Set of contingencies.
d	An onshore PCC.	D	A set of onshore PCCs.
δr	Section length.	Δs	Minimum acceptable sea floor rise.
e	Graph edge.	g	OWPP generator.
$\boldsymbol{G}$	Set of OWPP generators.	h	Hour.
H	Set of hours.	λ^*	A* penalty function co-efficient.
p	A coordinate (point).	P	Set of coordinates.
$P_\wedge$	Set of candidate OSS coordinates.	P^c	Set of probabilities of contingencies.
r	A shortest path.	R	Set of shortest paths.
ρ	Number of parallel lines.	S	Capacity (MVA).
S^{mx}	Maximum capacity.	S^c	Constrained capacity.
σ	Sea depth scalar.	T	Set of turbines.
$\boldsymbol{T_B}$	Set of initializing topologies.	$\boldsymbol{T_H^*}$	Set of optimized topologies.
tl	A transmission lines.	$\boldsymbol{TL}$	Set of transmission lines.
τ	Lifetime.	wd	Water depth.

This project has received funding from the CORDOBA project funded by Flanders Innovation Entrepreneurship (VLAIO) in the framework of the spearhead cluster for blue growth in Flanders (Blue Cluster) – Grant number HBC.2020.2722

I. Introduction

Offshore wind energy is one of the most promising carbon reducing technologies in our fight against climate change. It is estimated that in Europe alone 240 to 450 GW of offshore wind power will be required by 2050 to meet the targets set within the Paris Agreement [1], [2]. With a currently installed capacity of 28.4 GW and a 2030 goal of 60 GW, the European offshore wind industry is on a course of rapid development [3], [4]. It is essential that the long term planning tools required to support this growth are developed to properly equip decision makers and planners along the way.

The Offshore Wind Topology Optimization Problem (OWTOP) describes the problem of optimal offshore grid expansion. This has traditionally meant optimizing cable cost within the Medium Voltage (MV) collection grid and a single point to point High Voltage (HV) connection to the onshore Point of Common Coupling (PCC). This approach is a product of a development perspective that treats a concession in isolation from its surroundings. In the early days of the industry this was appropriate as the development of new concessions was often spaced out both geographically and in time. As the industry has matured, however, larger and larger areas consisting of multiple neighbouring concessions are being developed at an unprecedented rate. It has become apparent that a development model that considers the possible cost savings and increased reliability of a HV transmission network designed such that current and future offshore developments in the region are taken into account is needed.

To encourage the development of more coordinated HV grids offshore, the U.K., made steps in this direction in 2009 by introducing a new asset class, the Offshore Transmission Owner (OFTO) [5]. In Europe, an example of this shift is unfolding in Belgium, where decision makers are weighing options for expanding the Modular Offshore Grid (MOG) and building a multi functional energy island [6], [7].

Research into the optimal topology of the HV network is still quite limited [8]–[10] with a majority of work focused on the MV network [10]–[24]. In the case of projects like the MOG, however, the transmission infrastructure is planned prior to the finalization of concessions. As such, traditional OWTOP approaches that focus on Offshore Substation (OSS) location and cable length minimization in the context of the MV collection circuit layout are not directly applicable until a later stage of development is reached.

2023 IEEE Belgrade PowerTech | 978-1-6654-8778-8/23/$31.00 ©2023 IEEE | DOI: 10.1109/POWERTECH55446.2023.10202698

As the topology optimization problem is non linear and non convex with non continuous decision variables, it is classified as NP hard. There has been generally two avenues researchers have taken in developing approaches to the problem. The first is to apply a meta-heuristic to obtain a high quality but possibly sub-optimal solution within a reasonable computation time. The flexible structure of a meta-heuristic makes it relatively easy to capture a wide variety of problem characteristics, however, this advantage is gained at the expense of a certificate of global optimality. The most frequently applied meta-heuristic is a Genetic Algorithm (GA) [9]–[14] but a wide range of other algorithms have also been implemented including particle swarm [17], simulated annealing [19], modified bat algorithm [18], modified Clark and Wright's saving algorithm [20], minimum spanning tree [21], branch exchange [25] and path search [26].

The second approach is a more structured traditional mathematical formulation. This approach includes convex relaxations [27]–[29], stochastic programming [22], [23] and Mixed Integer Programs (MIPs) [8], [24]. This type of approach is desirable as a guarantee of global optimality can be obtained in many cases and if not, a minimum lower bound is calculated providing at least a measure of the solution quality. The drawback is that the rigid structure makes it difficult to realistically capture, in a single problem formulation, characteristics that have been shown essential to consider such as reliability [13], [15], the stochastic nature of wind [22], [23], [30] and optimal placement of OSS [12], [16], [20]. The final point regarding OSS placement is particularly challenging due to the limited number of binary variables ($<$10000) that are computationally tractable [8], [31].

In this work, bathymetry information is integrated directly into the electrical system optimization in order to reduce the search space for the position of OSSs and therefore the number of binary variables. Although this may appear obvious as OSS location is heavily constrained by the sea floor, it is not standard practise. To the best knowledge of the authors this is the first work providing an approach to the HV OWTOP that considers the bathymetry of the sea floor. The main contributions of this work are three fold:

1) A hybrid heuristic - mathematical optimisation formulation to solve OWTOPs.
2) A three dimensional spacial offshore grid planning model.
3) Proposed simplifications to the three dimensional spacial planning model.

The remainder of the paper is organized as follows. In the next section an overview of the optimization methodology and description of the optimization domain and economic model are provided. The algorithm developed for defining candidate OSSs is then presented. Following this, the required modifications to the greedy search algorithm [31] to handle the three dimensional spacial model are discussed. This includes the proposed three dimensional approximations. Then, the structure of a candidate topology based MIP formulation is presented. This formulation differs from the traditional Transmission Network Expansion Problem (TNEP) by considering candidate topologies rather than candidate equipment, resulting in a greatly reduced number of binaries and in turn increasing computational tractability. In the last section, an optimization of the transmission networks for the offshore wind development in the Belgian EEA is presented. The results from the full optimization process are compared to two implementations using the proposed three dimensional approximations. It is shown that for a small trade off in solution quality a large gain in computation time can be achieved.

II. Model

A. Methodology Overview

The developed approach is outlined in Fig. 1. There are four main steps in the optimization. First, the optimization domain is constructed and boundary inputs such as bathymetry, no-go zones, concessions, PCCs and wind power time series are defined. Second, a set of candidate OSSs locations are determined according to bathymetry and shortest paths between concessions and PCCs. In the third step the combinatorial search space of the problem is reduced using a greedy algorithm originally proposed in [31]. This results in a set of single export cable, radial topologies spanning the combinatorial space. These topologies are the input candidates for the MIP which finalizes the search for the optimal transmission system.

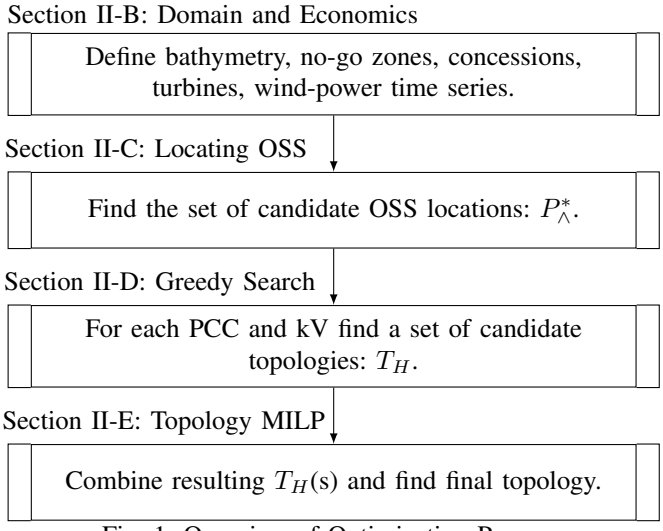

Fig. 1: Overview of Optimization Process.

B. Domain and Economics

The optimization domain consists of the Offshore Wind Power Plant (OWPP) concessions, turbines, associated wind power time series, PCCs, offshore bathymetry and no-go zones: which are areas where installation of transmission infrastructure is forbidden, such as military zones, dedicated shipping routes or nature protection zones. In the results section the optimization domain of the Belgian EEA is presented and illustrates the various aspects mentioned here.

The economic model is described in [31] and accounts for Capital Expenditures (CAPEX), cable and transformer losses, corrective maintenance and Expected Energy Not Transmitted (EENT). The offshore substation costs consider the power rating and number of parallel transformers, amount of reactive compensation and the medium and high voltage switch gear. For HV submarine cables, the cross section and number of parallel conductors are considered. EENT is calculated, considering n-1 reliability as in:

$$EENT = \tau \sum_{h \in H} \sum_{i \in C} (S_h - S_i^c) \cdot P_i^c. \quad (1)$$

Where τ is the project lifetime in years, C is the set of possible contingencies, H is the set of hours in a year, S_h is the power generated at time h, S_i^c is the constrained transmission capacity under contingency i and P_i is the probability of occurrence of contingency i. S_h is calculated using the CorWind software which combines meteorological data and stochastic simulations to provide a generation time series with a per hour resolution for each concession [32].

C. Locating OSS

1) Scalling cost with depth: The material and installation costs for foundations of offshore infrastructure increase with sea depth. In [33] a set of scale factors σ at four different water depths between 10 m and 50 m are derived. Using linear interpolation between the points results in the water depth dependent scale factor:

$$\sigma(wd) = 0.0136 \cdot (wd - 17) + 0.7676 \quad (2)$$

where wd is the water depth in meters.

2) Candidate OSS Algorithm: It is desirable to locate OSSs in a location that both minimizes the length of required collection and transmission cables and minimizes the cost of the substructure by building in as shallow an area as feasible. The developed algorithm searches in the vicinity of the optimal cable routing paths for elevated areas in the sea bed. The resulting set of candidate OSS locations are therefore both close to the optimal cable routes and at the highest feasible elevation. The algorithm is outlined below in steps (i) to (xi).

(i) For each OWPP concession i, find the centroid point g_i as in:

$$g_i = \frac{\sum_{p_i \in T_i} p_i}{k} \quad (3)$$

where T_i is the set of coordinates of the k turbines within the concession.

(ii) Using the A* algorithm [34], find the set of shortest routes R_{gd} connecting each point g_i to each PCC, d_i. A route $r_{g_i d_i} \in R_{gd}$ is comprised of a set of weighted edges e_{ij}, defined by a start and end point (p_i, p_j) and weight:

$$||e_{ij}|| = \sqrt{(p_{i_x} - p_{j_x})^2 + (p_{i_y} - p_{j_y})^2 + (p_{i_z} - p_{j_z})^2}. \quad (4)$$

(iii) From R_{gd} find the set of points P_{gd}. Point $p_i \in P_{gd}$ is both a point occurring in $r_{g_i d_i}$ and lying on the perimeter of OWPP concession i. Fig. 2 shows a generic concession, identifying points $p_i \in P_{gd}$, g_i, $p_i \in T_i$ and $r_{g_i d_i}$.

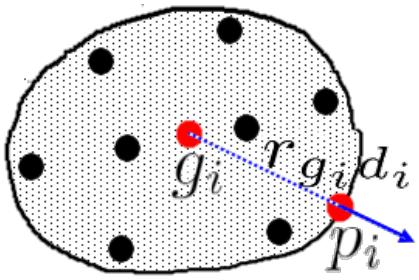

Fig. 2: Generic OWPP concession showing g_i, $r_{g_i d_i}$ and $p_i \in P_{gd}$. Unlabelled points are $p_i \in T_i$.

(iv) Update all paths $r_{g_i d_i} \in R_{gd}$ to start from $p_i \in P_{gd}$ discarding edges $e_{ij} \in r_{g_i d_i}$ occurring within $[g_i, p_i)$. In Fig. 2 the discarded section of the path is shown as a dotted line.

Steps (v) through $(viii)$ are analogous to steps (i) through (iv) but applied to connections between two OWPPs rather than an OWPP and PCC.

(v) Using the A* algorithm, find the set of shortest routes R_{gg} connecting each point $p_i \in P_{gd}$. A route $r_{g_i g_j} \in R_{gg}$ is comprised of a set of weighted edges e_{ij}, with weight calculated as in (4).

(vi) From R_{gg} find the set of points P_{gg}. Point $p_i \in P_{gg}$ is both a point occurring in $r_{g_i g_j}$ and lying on the perimeter of OWPP concession i. Due to the inherent symetry of the problem and by definition of a shortest path, $r_{g_i g_j} = r_{g_j g_i}$, both start and end points must be updated.

(vii) Update all paths $r_{g_i g_j} \in R_{gg}$ to start from $p_i \in P_{gg}$ discarding edges $e_{ij} \in r_{g_i g_j}$ occurring within $[p_i \in P_{gd}, p_i \in P_{gg})$ or $[p_j \in P_{gd}, p_j \in P_{gg})$. This must be applied to both ends of the path.

$(viii)$ Define the set of all shortest paths as $R = R_{gd} \cup R_{gg}$.

(ix) From R find set $P_\wedge$ where $p_i \in P_\wedge$ is the shallowest point within a route section of length δr. δr is an adjustable parameter. Smaller values of δr result in a higher number of candidate OSSs locations that are closely spaced.

(x) For each point $p_i \in P_\wedge$ search an area of 2D Euclidian radius δr for point(s) p_j that satisfy the condition:

$$\frac{p_{j_z} - p_{i_z}}{\sqrt{(p_{i_x} - p_{j_x})^2 + (p_{i_y} - p_{j_y})^2}} \geq \Delta s_{mn}. \quad (5)$$

Δs_{mn} is an adjustable parameter that defines the minimum sea floor rise per unit horizontal distance required to justify moving the OSS location away from the shortest path. An example of choosing an appropriate Δs_{mn} is provided in the results section. For each p_j satisfying (5), p_j replaces $p_i \in P_\wedge$. Only unique points are maintained in $P_\wedge$.

(xi) Step (x) is repeated until no further points p_j satisfying condition (5) are found. The resulting set $P^*_\wedge$ is the desired set of all candidate OSS locations.

3) A route finding and penalty function:* Installing transmission cables through the MV networks of neighboring concessions is often avoided. To that end, a penalty function is added to the A* route finding algorithm. The penalty function increases the cost of any edge, e_{ij}, within a region where it is undesirable to install HV cable, such as a neighboring concession, by a factor λ^*. λ^* for neighboring concessions is defined as the ratio of the perimeter over the longest straight line cut through the concession. λ^* is 1 for the source and destination OWPPs. Setting the value of λ^* to 1 for all OWPPs results in a standard implementation of the A* algorithm.

D. Greedy Search

In [31] a greedy algorithm is developed that efficiently searches the combinatorial space describing the possible OWPP interconnections. As part of the algorithm a formal mathematical representation of the search space is derived, whereby combinations of OWPPs are represented by binary strings. The details of this algorithm are out of the scope of this paper and only a very brief intuitive explanation is provided in the following. For further details the authors refer readers to the original paper. As the algorithm has been modified to consider the spacial details of the offshore zones including bathymetry, these modifications are also discussed in the following paragraphs.

The greedy search is initialized by an input set of topologies $\boldsymbol{T_B}$. Set $\boldsymbol{T_B}$ contains a base topology for each possible combination of OWPPs connected through a single export cable to the PCC. Fig. 3 gives a visual representation of $\boldsymbol{T_B}$ for a four OWPPs case. The location of the OSS is defined by minimizing the total cost of the connected cabling. In fig. 3 the binary string representation of each connection is included below the topology. The length of set $\boldsymbol{T_B}$ is $2^n - 1$ where n is the number of OWPPs.

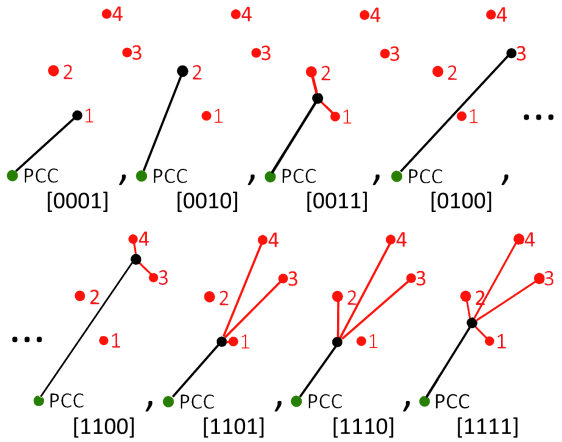

Fig. 3: An exemplary $\boldsymbol{T_B}$ for a 4 OWPP cluster. The OWPPs are red dots, the OSS black dots, MV cables are red and HV cables are black. [31]

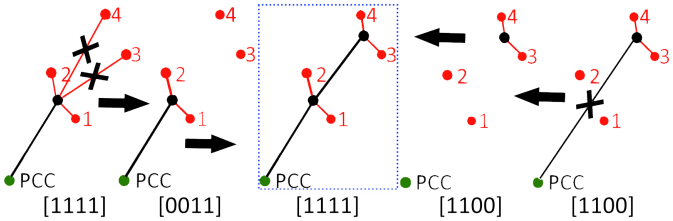

Fig. 4: Greedy search cross over. [31]

Starting with input $\boldsymbol{T_B}$, the greedy search algorithm finds the set $\boldsymbol{T^*_H}$. Set $\boldsymbol{T^*_H}$ is the set of $2^n - 1$ optimal radial topologies connected to the PCC via a single export cable. Set $\boldsymbol{T^*_H}$ is found via a process of deterministic cross over of the topologies. Fig. 4 presents an example of a single cross over performed by the greedy search. The binary string representation below the topologies demonstrates how it is ensured that cross-overs always result in a valid topology. When a new lower cost topology is found it replaces the previous topology of the same binary string. Cross overs are performed unidirectionally, starting at the first element of $\boldsymbol{T_B}$ and ending at the $2^n - 1^{th}$ element. For a single transmission voltage the algorithm is guaranteed to find the global optimal for each combination (binary string) of OWPPs. The correctness of the greedy search algorithm is ensured via the greedy stays ahead principle, a proof is provided in [31].
Adapting the algorithm to include bathymetry is quite straight forward. Calculated locations of OSSs are moved to the lowest cost location within $P^*_\wedge$, resulting in an OSS location that is both in shallow water and near the optimal location with regards to cable length. If no location within $P^*_\wedge$ results in a lower cost topology then the position remains unchanged. Once the positions of the OSS are calculated, three dimensional cable lengths are calculated using the A* route finding algorithm as described previously.

Approximating the 3rd dimension in large systems: The three dimensional problem introduces the additional computational burden of solving the route finding problem for every candidate cable length considered. This is computationally expensive as the bathymetry graph size can be very large. For example, the bathymetry data for the Belgian offshore region discussed later on, has a resolution of 20m by 20m and results in over 2^{14} data points. The resulting network graph, after eliminating no–go regions still contains well over 32 million edges. Each shortest path calculation on a graph of this size takes about 10 to 15 seconds in the Julia language [35] using the light graphs [36] implementation of A*. This has a substantial impact on computation time and makes some larger problem sizes intractable. To deal with these cases two 3D approximations are proposed.
The first, termed (A1), approximates the length of the 3D path from the 2D Euclidean distance. (A1) employs a look up table of multipliers as in Table I. This table can be calculated with no extra computational burden while finding the optimal OSS locations of $P^*_\wedge$. Table I converts a 2D Euclidean distance to an approximation of the 3D route by multiplying by the table

TABLE I: Multipliers for 3D approximation.

	g_1	...	g_n	PCC1	...	PCCN
g_1	1	...	$\frac{l^{3d}_{1n}}{l^{2d}_{1n}}$	$\frac{l^{3d}_{1d_1}}{l^{2d}_{1d_1}}$	...	$\frac{l^{3d}_{1d_n}}{l^{2d}_{1d_n}}$
...	...	...	...	...	...	...
g_n	$\frac{l^{3d}_{n1}}{l^{2d}_{n1}}$	...	1	$\frac{l^{3d}_{nd_1}}{l^{2d}_{nd_1}}$	...	$\frac{l^{3d}_{nd_n}}{l^{2d}_{nd_n}}$
PCC1	$\frac{l^{3d}_{d_11}}{l^{2d}_{d_11}}$	...	$\frac{l^{3d}_{d_1n}}{l^{2d}_{d_1n}}$	1	...	n/a
...	...	...	...	...	...	...
PCCN	$\frac{l^{3d}_{d_n1}}{l^{2d}_{d_n1}}$	...	$\frac{l^{3d}_{d_nn}}{l^{2d}_{d_nn}}$	n/a	...	1

entry with the column and row entries that match closest to the source and destination nodes of the 2D distance.

A second approximation, termed (A2), estimates the distance from the centroid of a concession to the optimal MV-HV connection point. When solving A* in the full 3D problem, these points are found explicitly as they are the points within the shortest path that also lie on the perimeter of the source and destination concessions. (A2) approximates this distance by the average radius of the target concession. As concessions are not perfect circles the radius is defined as the average distance between a cluster's centroid and points along its perimeter.

E. Topology MILP

In a traditional MIP formulation for grid expansion, such as the TNEP formulation, the binary decision variables are assigned to single candidate equipment, such as cables and transformers. As the feasible problem size is strongly dependent on the number of binary variables, the tractable problem size is severely limited with this approach. In this section a MIP formulation is presented where a single binary variable represents a complete topology appearing within $\boldsymbol{T^*_H}$.

$\boldsymbol{G}$ is a set of n OWPPs g_i each with a maximum generating capacity of S^{mx}_i and $\boldsymbol{D}$ is a set of m PCCs with a variable demand between S^{mn}_k and S^{mx}_k as in:.

$$\begin{gathered}\boldsymbol{G} = \{g_i \in \mathbb{Z}^+_0 \mid g_i < n\}\\ \boldsymbol{D} = \{d_k \in \mathbb{Z}^+_0 \mid d_k < m\}\\ S_i = S^{mx}_i \text{ and } S^{mn}_k \leq S_k \leq S^{mx}_k.\end{gathered} \tag{6}$$

$\boldsymbol{B}$ is a set of auxiliary buses. There is one auxiliary bus for each topology j in $\boldsymbol{T^*_H}$. Each auxiliary bus b_j is represented by an n-length binary string, such that a value of one only occurs at the bit position equal to i if OWPP g_i is connected within the topology j:

$$\boldsymbol{B} = \{b_j \in \mathbb{N}^n_2 \mid b_j = \sum_{g_i \in j} 2^i, \forall j \in \boldsymbol{T^*_H}\} \tag{7}$$

$\boldsymbol{TL^b}$ is a set of transmission lines, tl^b_{ij}, connecting OWPP g_i to an auxiliary bus b_j with maximum transmission capacity S^{mx}_{tl}, equal to the generating source S_i:

$$\begin{gathered}\boldsymbol{TL^b} = \{tl^b_{ij} \; \forall (i=1) \in b_j \text{ and } \forall b_j \in \boldsymbol{B}\}\\ 0 \leq S^b_{ij} \leq S_i.\end{gathered} \tag{8}$$

$\boldsymbol{TL^{\mathbb{B}}}$ is a set of transmission lines, $tl^{\mathbb{B}}_{jk}$, connecting auxiliary bus b_j to PCC d_k with maximum transmission capacity S^{mx}_{tl}, equal to the sum of generation connected to b_j. For each transmission line $tl^{\mathbb{B}}_{jk}$, there exists a decision variable $\mathbb{B}_{jk} \in \boldsymbol{\mathcal{B}}$ and cost $\mathbb{C}_{jk} \in \boldsymbol{\mathcal{C}}$:

$$\begin{gathered}\boldsymbol{TL^{\mathbb{B}}} = \{tl^{\mathbb{B}}_{jk}\}, \boldsymbol{\mathcal{B}} = \{\mathbb{B}_{jk} \in \{0,1\}\},\\ \boldsymbol{\mathcal{C}} = \{\mathbb{C}_{jk} \in \mathbb{R}\} \mid \forall d_k \in j \text{ and } \forall b_j \in \boldsymbol{B}\\ 0 \leq S^{\mathbb{B}}_{jk} \leq \sum_{g_i \in j} S_i\end{gathered} \tag{9}$$

The objective of the optimization is to minimize the total cost of transmission lines

$$min(\sum_{\boldsymbol{\mathcal{B}},\boldsymbol{\mathcal{C}}} \mathbb{B}_{jk} C_{jk}) \tag{10}$$

such that all system capacity limits are respected and the net power flow at any node is zero:

$$\begin{gathered}\sum_{j \in \boldsymbol{TL^b}} S^b_{ij} = S_i \mid \forall g_i \in \boldsymbol{G}\\ \sum_{i \in \boldsymbol{TL^b}} S^b_{ij} = S^{\mathbb{B}}_{jk} \mathbb{B}_{jk} \mid \forall b_j \in \boldsymbol{B}\\ \sum_{j \in \boldsymbol{TL^{\mathbb{B}}}} S^{\mathbb{B}}_{jk} \mathbb{B}_{jk} = S_k \mid \forall d_k \in \boldsymbol{D}\end{gathered} \tag{11}$$

Since $\boldsymbol{T^*_H}$ is the set consisting of all optimal radial topologies with a single export cable for each of the $2^n - 1$ combinations, it is easy to show that the topology found by the MIP is the globally optimal radial topology with $1 \leq \rho \leq n$ export cables. The proof of this is as follows.

Given the constraint that no meshed connections are permitted, we name the optimal topology connecting n OWPPs with k PCC as j^*. Since j^* has ρ export cables, it can be written as the union of ρ independent radial topologies, each with a single connection to a PCC k, as in:

$$j^* = \bigcup_{j=1}^{\rho} j \mid \sum_{g_i \in j_1}^{j_\rho} 2^i = 2^n - 1 \tag{12}$$

Since the cost of j^* is the sum of the costs of the ρ independent topologies, j, it follows that for j^* to be optimal each of the ρ radial topologies must also be optimal and therefore members of $\boldsymbol{T^*_H}$.

III. Case Study - Belgian Exclusive Economic Area

In this section a possible design for the offshore wind power plant connections of the Belgian EEA is found using the proposed method. A 25 year lifetime is assumed at a discount rate of 4% [37]. All bathymetry and marine spatial planning data is obtained from the Flemish Hydrography, Coastal Division, Agency for Maritime and Coastal Services [38]. In addition to the full size problem, the proposed approximations are analyzed and the resulting topologies and computation times are compared.

OWPP	1	2	3	4	5	6	7	8
MVA	290	310	270	270	190	180	290	270
OWPP	9	10	11	12	13	14	15	16
MVA	330	380	370	360	320	310	260	170

TABLE II: Capacities of individual concessions within zones 1, 2 and 3 of the Belgian offshore.

Optimization Domain

The layout of the OWPP concessions in zones 1, 2 and 3 in Fig. 5 are modeled by clustering the x and y coordinates using k-means clustering, setting $k = 16$ as the desired total number of concessions. The sixteen resulting concessions, three zones, two PCCs and bathymetry spanning the Belgian domain are shown in Fig. 5. The PCCs are in Zeebruges and Oostende, labelled A and B respectively. The maximum capacity that can be connected to any single PCC is assumed to be 3 GW. The white crosses shown, are underwater obstacles such as ship wrecks that must be avoided. Regions off limit to electrical infrastructure are left as blank, white areas.

Turbines, shown in the figure as dots in the parent concession's colour, have a capacity of 10 MW and are evenly spaced considering a power density of 9.5 MW/km^2. A buffer zone for cable laying and ship traffic of two times the turbine spacing ($\approx$ 2 km) is guaranteed between neighbouring concessions. The resulting generation capacity of the entire Belgium EEA is 4.57 GW. Individual concession capacities are in Table II.

OSS Candidates

With the domain defined, the next step is to calculate the candidate OSS locations, $P^*_\wedge$, as in section II-C. These locations, considering only PCC-A, are shown in Fig. 6 as white crosses. In addition, the set of shortest routes $R = R_{gd} \cup R_{gg}$ are displayed as black lines. R_{gd} are the routes connecting OWPPs to the PCCs and R_{gg} connect OWPPs to other OWPPs. From R, considering a δr of 1 km, $P_\wedge$ is found and then the final set of candidate OSS locations, $P^*_\wedge$, follows by iteratively applying condition (5) until convergence.

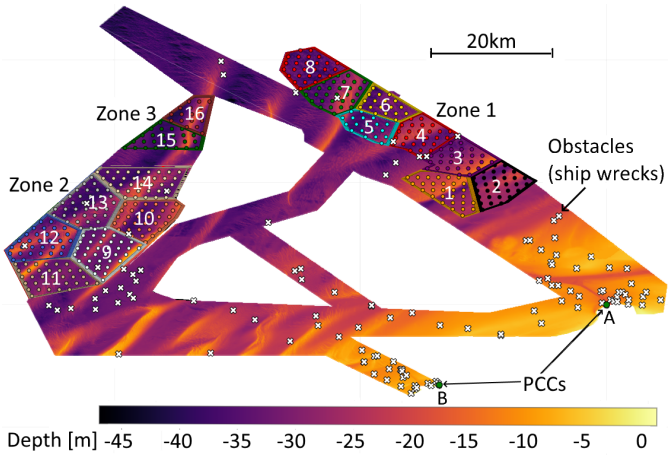

Fig. 5: Belgian EEA bathymetry, sea based renewables regions 1, 2 and 3, designated cable ways, PCCs and under water obstacles.

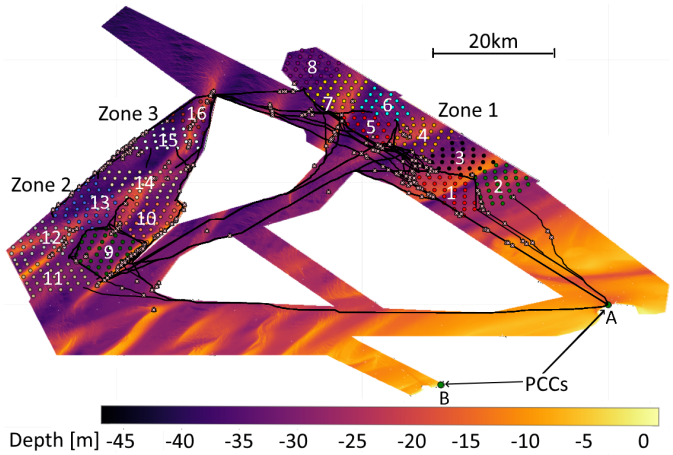

Fig. 6: Belgian Offshore - Shortest paths and candidate OSS locations.

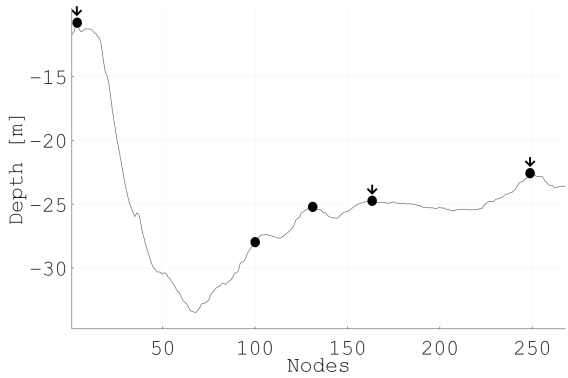

Fig. 7: variation in sea depth along the first 5.5 km of the shortest path from g_3 to the PCC-A.

This process is demonstrated on a section of the bathymetry from the first 5.5 km of the route connecting g_3 to the PCC in Fig. 7. The initial set of points, $P_\wedge$, are all five of the black dots shown. However, only those indicated by an arrow satisfy condition (5) and are therefore included in the final set of candidate OSSs locations: $P^*_\wedge$.

Condition (5) is dependant on parameter Δs_{mn}, the minimum acceptable rise in the sea floor per distance travelled that justifies a change in the position of the OSS. The optimal value of Δs_{mn} is situation specific and varies given the number, capacity and relative orientation of OWPPs connected to the OSS. An approximate range for Δs_{mn} lies between 0.5 and 2.5 m/km and it is inversely proportional to the number of connected OWPPs. This is the case as when the number of OWPP feeders connected to the OSS increases, OSS movement causes certain feeders to increase in length and others to decrease, offsetting the overall impact on cost. The same logic explains why the highest value of Δs_{mn} occurs when only a single OWPP feeder is connected to the OSS. In this work, a value of 1.4 m/km is used. This is the break even slope for OWPPs 1, 2, 3 and 4 connected to single OSS.

Optimal Solution

The hybrid greedy - MIP optimization finds an optimal topology of cost 2285.6 M€ which is shown in Fig. 8. Four OSSs are built and have been located in water depths of 12 m or less. The OSSs from A to D have capacities of 540 MVA, 930 MVA, 1760 MVA and 740 MVA respectively. Four export cables at 220 kV connect the OSSs to the PCCs. Zone 1 OWPPs are only connected to PCC-A while zones 2 and 3 OWPPs are only connected to PCC-B. OWPPs 1 and 2 in zone 1 are connected to shore at 66 kV. All MV collection circuit connection points are at the point within the concession that minimizes the length of transmission cable. The distribution of costs are shown in table III, of which the CAPEX is slightly over three quarters of the entire cost.

3D Approximations

The problem is again optimized while implementing the 3D approximations as follows:

1) Only approximation (A1) is used to estimate 3D route length from the 2D Euclidean length. When necessary to calculate an MV to HV connection point the route finding algorithm is used.
2) Both approximation (A1) and (A2) are used. The route finding algorithm is only implemented when calculating $P^*_{\wedge}$ and for the final solution topology of the MIP.

The optimal topology found when using only approximation (A1) is identical to that of the full problem, indicating the approximation of HV cable length does not introduce significant error for the studied case. When using both approximations (A1) and (A2), however, a slight degradation of the solution topology is noted. Although the topology only costs 1.1 % more than that of the full size problem. This is less than the uncertainty within the economic model. It demonstrates that approximating the MV connection point by the average radius introduces enough error to alter the final topology selection. The topology from (A1)+(A2) is shown in Fig. 9. As can be seen the solution in zones 2 and 3 is identical to the full size problem. In zone 1, again two OSSs are built, however, OSS A is in a different location and both are of a smaller capacity. OSS A is 460 MVA and OSS B; 740 MVA. Transmission is accomplished at 220 kV. The smaller OSSs are possible as OWPP 3 in addition to 1 and 2 are connected to shore at 66 kV.

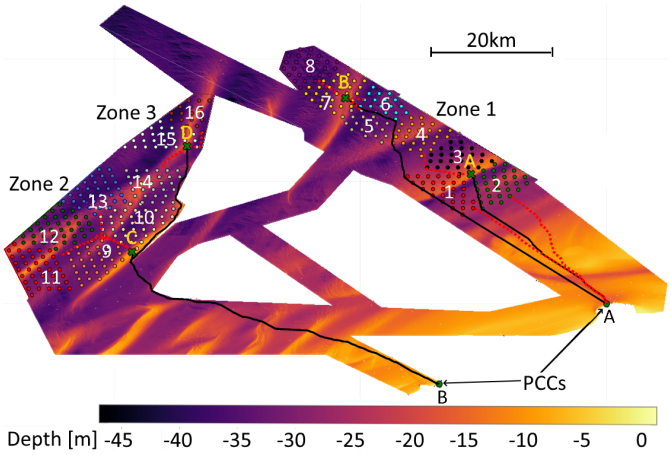

Fig. 8: Optimal Solution for the Belgian EEA. 220 kV cables are shown in black while 66 kV cables in red.

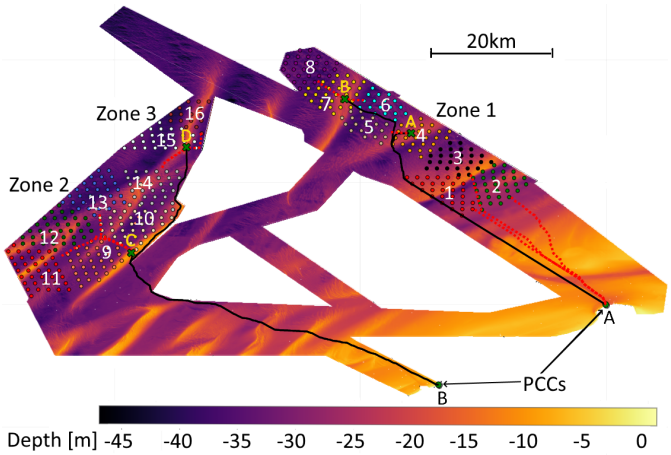

Fig. 9: Optimal Solution for the Belgian EEA using approximations (A1) and (A2). 220 kV cables are shown in black while 66 kV cables in red.

In table IV the computational times of the full problem and the approximations are compared. The full problem requires twice as much computation time compared to (A1) and 76.5 times more than (A1)+(A2). Since in planning problems computational burden is not of high priority the approximations are only necessary when the full size problem becomes intractable. It is important to note that computational times include scenarios at both 400 kV and 220 kV as well as possible connections to either PCC of any OWPP. The calculation of $\boldsymbol{T}^*_{\boldsymbol{H}}$, the most computationally intensive aspect, is completely independent in each of these scenarios and so the problem can be easily decomposed into parallel calculations. In the Belgian case this reduces overall computation time by a factor of four.

IV. Conclusions

A methodology for finding the optimal HV transmission topology considering multiple onshore connection points,

TABLE III: Objective function values for the 3 optimizations.

	Total [M€]	CAPEX [M€]	OPEX [M€]
Full/A1	2285.6	1737.5	548.1
A1+A2	2311.5	1741.7	569.8

CAPEX: Procurement and Installation.
OPEX: Corrective Maintenance, EENT and Losses.

TABLE IV: Comparison of computation times in minutes.

	Full	(A1)	(A1)+(A2)
Domain	40.2	40.2	40.2
$\boldsymbol{T}^*_{\boldsymbol{H}}$	6720.1	3035.2	44.3
MIP	0.2	0.2	0.2
Post Process	3.7	3.7	3.7
Total	6764.2	3079.32	88.4

bathymetry, no-go zones and full wind power generation time series has been presented. The methodology combines an original candidate OSS search algorithm based on the shortest route finding algorithm A*, a combinatoric greedy search algorithm and a MIP to optimize the offshore network. As both the greedy search and MIP have guarantees of global optimality associated to their respective solutions, a high solution quality is guaranteed. To demonstrate the effectiveness of the approach a case study of the Belgian EEA is presented. In addition, two approximations for the computationally intensive 3D route finding problem are suggested and the results compared to the full size problem. The approximations are shown to result in high quality solutions, only 1.1% more expensive in the worse case, while reducing computational burden by up to 76 times.

REFERENCES

[1] "The Paris Agreement," United Nations Treaty Collection XXVII 7.d.

[2] *The European Green Deal: delivering step by step*. Luxembourg: Publications Office, 2020.

[3] Rebecca Williams, Feng Zhao, Joyce Lee, "Global Offshore Wind Report 2022." World Forum Offshore Wind., Tech. Rep., 2022.

[4] Baldock, "National energy and climate plan 2021-2030," Belgian Federal Government Consultation Committee, Tech. Rep., 2019.

[5] Cox et al. - KPMG LLP, "Offshore Transmission: An Investor Perspective - Update Report," https://www.ofgem.gov.uk, accessed: 20-06-18.

[6] P. Sorensen, M. Koivisto, J. Murcia, "Final study report: MOGII System integration study," Elia Transmission Belgium, DTU Wind Energy, Tech. Rep., 2020.

[7] B. Smith, "EU ALL for Belgian Energy Island," https://www.4coffshore.com/news/eu-all-for-belgian-energy-island-nid23751.html, accessed: 2021-07-17.

[8] S. Hardy, H. Ergun, D. Van Hertem, K. Van Brusselen, "A Techno-Economic MILP Optimization of Multiple Offshore Wind Concessions." *Large-Scale Grid Integration of Renewable Energy in India*, 2019.

[9] H. Ergun, D. Van Hertem, and R. Belmans, "Transmission System Topology Optimization for Large-Scale Offshore Wind Integration," *IEEE transactions on sustainable energy*, vol. 3, no. 4, pp. 908–917, 2012.

[10] H. Lingling, F. Yang, and G. Xiaoming, "Optimization of electrical connection scheme for large offshore wind farm with genetic algorithm," pp. 1–4, 2009.

[11] J. Gonzalez, A. Rodriguez, J. Mora, J. Santos, and M. Payan, "A new tool for wind farm optimal design," pp. 1–7, 2009.

[12] Dahmani et al., "Optimization of the connection topology of an offshore wind farm network," *IEEE. Syst. J. 2015*, no. 9, p. 1519–1528, 2015.

[13] O. Dahmani, S. Bourguet, M. Machmoum, P. Guerin, P. Rhein, and L. Josse, "Optimization and Reliability Evaluation of an Offshore Wind Farm Architecture, copyright = Copyright 2017 Elsevier B.V., All rights reserved." *IEEE transactions on sustainable energy*, vol. 8, no. 2, pp. 542–550, 2017.

[14] A. M. Jenkins, M. Scutariu, and K. S. Smith, "Offshore wind farm inter-array cable layout," in *2013 IEEE Grenoble Conference*, 2013, pp. 1–6.

[15] O. Dahmani, S. Bourguet, M. Machmoum, P. Guerin, and P. Rhein, "Reliability analysis of the collection system of an offshore wind farm," in *2014 Ninth International Conference on Ecological Vehicles and Renewable Energies (EVER)*. IEEE, 2014, pp. 1–6.

[16] P. Hopewell, F. Castro-Sayas, and D. Bailey, "Optimising the Design of Offshore Wind Farm Collection Networks," in *Proceedings of the 41st International Universities Power Engineering Conference*, vol. 1. IEEE, 2006, pp. 84–88.

[17] X. Gong, S. Kuenzel, and B. C. Pal, "Optimal Wind Farm Cabling," *IEEE Transactions on Sustainable Energy*, vol. 9, no. 3, pp. 1126–1136, 2018.

[18] P. Hou, W. Hu, C. Chen, and Z. Chen, "Optimisation of offshore wind farm cable connection layout considering levelised production cost using dynamic minimum spanning tree algorithm," *IET renewable power generation*, vol. 10, no. 2, pp. 175–183, 2016.

[19] S. Lehmann, I. Rutter, D. Wagner, and F. Wegner, "A Simulated-Annealing-Based Approach for Wind Farm Cabling," in *Proceedings of the Eighth International Conference on Future Energy Systems*, ser. e-Energy '17. New York, NY, USA: Association for Computing Machinery, 2017, p. 203–215. [Online]. Available: https://doi.org/10.1145/3077839.3077843

[20] T. Zuo, Y. Zhang, K. Meng, and Z. Y. Dong, "Collector System Topology for Large-Scale Offshore Wind Farms Considering Cross-Substation Incorporation," *IEEE Transactions on Sustainable Energy*, pp. 1–1, 2019.

[21] Y. Qi, P. Hou, L. Yang, and G. Yang, "Simultaneous optimisation of cable connection schemes and capacity for offshore wind farms via a modified bat algorithm," *Applied sciences*, vol. 9, no. 2, p. 265, 2019.

[22] M. Banzo and A. Ramos, "Stochastic optimization model for electric power system planning of offshore wind farms," *IEEE transactions on power systems*, vol. 26, no. 3, pp. 1338–1348, 2011.

[23] S. Lumbreras and A. Ramos, "A Benders' Decomposition Approach for Optimizing the Electric System of Offshore Wind Farms," *IEEE Trondheim PowerTech conference*, 2011.

[24] J. Bauer and J. Lysgaard, "The offshore wind farm array cable layout problem: a planar open vehicle routing problem," *Journal of the Operational Research Society*, vol. 66, no. 3, pp. 360–368, 2015. [Online]. Available: http://www.tandfonline.com/doi/abs/10.1057/jors.2013.188

[25] Edelmiro et al., "An Improved Branch-Exchange Algorithm for Large-Scale Distribution Network Planning," *IEEE transactions on power systems*, 2002.

[26] Vikrant et al., "Optimization of Radial Distribution Networks Using Path Search Algorithm," *International Journal of Electronics and Electrical Engineering*, 2013.

[27] J. A. Taylor and F. S. Hover, "Convex Models of Distribution System Reconfiguration," *IEEE Transactions on Power Systems*, vol. 27, no. 3, pp. 1407–1413, 2012.

[28] H. Ergun, J. Dave, D. Van Hertem, F. Geth, "Optimal Power Flow for AC/DC Grids: Formulation, Convex Relaxation, Linear Approximation and Implementation," *IEEE Transactions On Power Systems*, vol. 34, no. 4, 2019.

[29] J. Dave, H. Ergun, and D. V. Hertem, "Relaxations and approximations of hvdc grid tnep problem," *Electric power systems research*, vol. 192, p. 106683, 2021.

[30] S. Lumbreras and A. Ramos, "Offshore wind farm electrical design: a review," *Wind Energy*, vol. 16, no. 3, pp. 459–473, April 2013.

[31] S. Hardy, H. Ergun, D. Van Hertem, "A Greedy Algorithm for Optimizing Offshore Wind Transmission Topologies." *IEEE Transactions on Power Systems*, 2021.

[32] M. Koivisto, K. Das, F. Guo, P. Sørensen, E. Nuño, N. Cutululis, P. Maule, "Using time series simulation tools for assessing the effects of variable renewable energy generation on power and energy systems," *Wiley Interdisciplinary Reviews: Energy and Environment*, vol. 8, no. 3, p. e329, 2019. [Online]. Available: https://onlinelibrary.wiley.com/doi/abs/10.1002/wene.329

[33] EEA, "Europe's onshore and offshore wind energy potential an assessment of environmental and economic constraints," European Environmental Agency, Tech. Rep., 2009.

[34] P. E. Hart, N. J. Nilsson, and B. Raphael, "A formal basis for the heuristic determination of minimum cost paths," *IEEE transactions on systems science and cybernetics*, vol. 4, no. 2, pp. 100–107, 1968.

[35] J. Bezanson, A. Edelman, S. Karpinski, and V. B. Shah, "Julia: A fresh approach to numerical computing," *SIAM review*, vol. 59, no. 1, pp. 65–98, 2017. [Online]. Available: https://doi.org/10.1137/141000671

[36] J. F. S Bromberger, "Juliagraphs/lightgraphs.jl: an optimized graphs package for the julia programming language," 2017. [Online]. Available: https://doi.org/10.5281/zenodo.889971

[37] Flament et al., "North Sea Grid, Final Report." 3E, Tech. Rep., 2014.

[38] Coastal Division - Flemish Hydrography. Belgian hydrography data. [Online]. Available: https://bathy.agentschapmdk.be/spatialfusionviewer/mapViewer/map.action